Two-Dimensional Hydrodynamic Characteristics of a Bluff Symmetrical Fairing Section

D. E. Calkins*
University of Washington, Seattle, Washington

An experimental wind-tunnel investigation has been conducted to determine the aero/hydrodynamic characteristics of bluff symmetrical sections with high thickness/chord ratios. The sections are used as fairings for circular cylindrical members, such as towing cables and offshore drilling rig riser pipes, which are deeply immersed in the ocean environment so that they are cavitation free. The fairings serve to reduce drag and lateral vibrations due to vortex shedding. The section tested had a 40% thickness/chord ratio and was designed for a Stratford pressure recovery. Measurements included the two-dimensional drag coefficient, chordwise neutral stability point, yaw torque about the pivot center, and boundary-layer transition and separation location.

Introduction

MARINE applications of line structures (high length/diameter ratio) with circular cylindrical sections include moored and towed cable systems, risers for offshore drilling rigs, and the "cold-water pipe" for the ocean thermal energy conversion (OTEC) system. All of these systems experience relative motion between the line structure and the surrounding water, due to either ship motion or current and wave motion. Because of this relative motion, the line structure experiences unsteady (time-dependent) hydrodynamic forces due to vortex shedding. When the frequency for the vortex shedding is close to the natural frequency of the line structure, a resonant structural response condition will occur. This resonant condition will increase the drag force (the force parallel to the current field), which in turn will result in cyclic motions and stresses.

One solution to the shed vortex problem is to fair the circular cylinder with a streamlined shape. An obvious drawback is that the fairing will act as a wing and generate large transverse lift forces unless it is allowed to swivel freely and align itself with the flowfield. However, this in turn dictates that the position of the hydrodynamic (aerodynamic) center must be aft of the mechanical center of rotation (the central axis of the line structure) for weathervane stability.

It should be noted that the hydrodynamic center, or neutral stability point, is used rather than the center of pressure. The hydrodynamic center is defined as the position along the chord about which the moment coefficient is constant independent of the lift coefficient, while the center of pressure position varies with the lift coefficient. For symmetrical sections, this constant-moment coefficient has a value of zero. The neutral point is defined as the point along the chord where the slope of pitching moment coefficient vs lift coefficient curve is zero. Therefore, the terms hydrodynamic center and neutral point are synonymous for a symmetrical section and are used interchangeably.

Problem Statement

Rigid symmetrical fairings in short lengths are presently commercially available from Fathom Oceanology Ltd. for application to towing cables, see Fig. 1. The fairings range in size from chord lengths of 5-15 cm for towing cable applications to 2 m for a drill pipe riser.[1] Hydrodynamic problems with the towing cable fairings have been encountered, as discussed by Henderson.[2] A fairing section that had a thickness/chord ratio (t/c) of 25% was found to have a hydrodynamic center position at the 15.4% chord position, which was aft of the center of rotation by a distance of only 2.3 mm (2.9% chord). It was determined experimentally that boundary-layer separation over the aft portion of the section caused the problem. The addition of a flat-plate trailing-edge extension, used to fix the position of the aft stagnation point, increased the chord to 100 mm and resulted in the movement of the hydrodynamic center to the 25% chord position.

The effect of t/c on the position of the aerodynamic center position was determined in the wind tunnel for the NACA 00-XX series section,[3] see Fig. 2. It is seen that the position of the aerodynamic center (in percent chord) moves forward toward the leading edge with increasing thickness-to-chord ratio, which is in qualitative agreement with the findings of Ref. 1.

The large diameters of line structures such as drill riser pipes (about 6.5-10 m) require that the fairing chord length be as small as possible for handling and installation considerations. This requirement results in fairing sections with very high thickness-to-chord ratios (up to 50%). Boundary-layer separation was apparently also observed in a series of wind-tunnel tests[4] on high thickness/chord ratio (0.4-0.5 c) fairings designed for riser lines. It was observed that the fairing did not possess weathervane stability. In this particular application, the problem was solved by the addition of fins to the fairing trailing edge, which acted like a split flap and stabilized the fairing.

Problem Solution

The selection of an optimum airfoil section shape for use as a fairing must include consideration of the following:

1) Streamlined symmetrical section for low drag.

2) Position of maximum thickness/chord as close to the leading edge as possible to keep center of rotation forward of hydrodynamic center for weathervane stability.

3) High thickness/chord ratio (bluff) sections to reduce the size of the fairings.

4) Separation-free boundary layer.

The utilization of bluff sections as fairings will lead to problems with boundary-layer separation, as already noted. Some means must therefore be used to prevent or control boundary-layer separation and to provide rotational stability. Three techniques present themselves as appropriate solutions,

Presented as Paper 82-0961 at the AIAA/ASME Third Joint Thermophysics, Fluids, Plasma and Heat Transfer Conference, St. Louis, Mo., June 7-11, 1982; submitted July 9, 1982; revision received Oct. 27, 1983.

*Research Associate Professor, Ocean Engineering Program, Department of Mechanical Engineering. Member AIAA.

either separately or synergistically: the use of separation-resistant sections and vortex generators for boundary-layer control and trailing-edge wedges for stability.

Recent advances in the development of boundary-layer separation-resistant airfoil sections with specified pressure profiles have shown some interesting results. A section with a 53.6% t/c (designed by Liebeck)[5] is the result of shaping the forward position of the section so that the pressure gradient is favorable to the laminar flow and then using the Stratford pressure recovery over the rear portion for separation control.

A passive technique for controlling the boundary layer is the use of vortex generators. This technique relies on the increased mixing between the external stream and the boundary layer as promoted by vortices trailing longitudinally over the surface from the generators. Vane-type generators are the ones most often used. They consist of a row of small plates that project normal from the surface with each set at an angle of incidence to the local flow to produce a single trailing vortex.

The use of "split-flap" wedges on the trailing edge of rudders has been investigated as a means to control the hydrodynamic moment.[6] This suggests itself as a technique that might have application for the fairing configuration to achieve rotational stability.

Experimental Investigation

The use of a wind tunnel for characterizing the hydrodynamics of the fairing section is appropriate, as long as Reynolds number equivalence is maintained. If it is assumed that the fairing section is being operated at depths

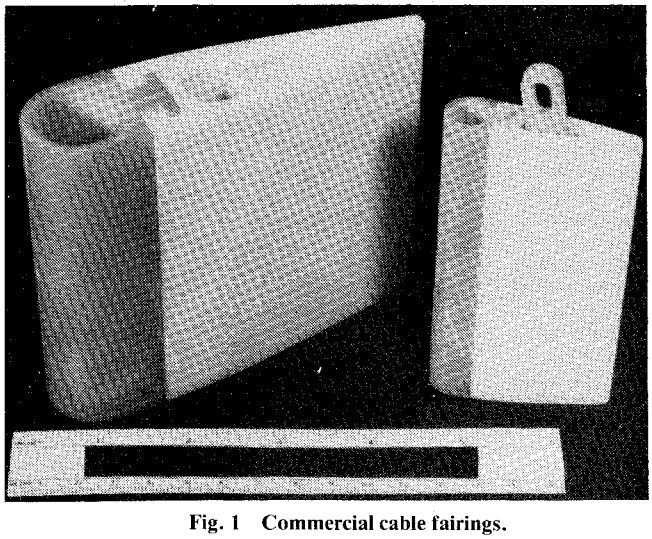

Fig. 1 Commercial cable fairings.

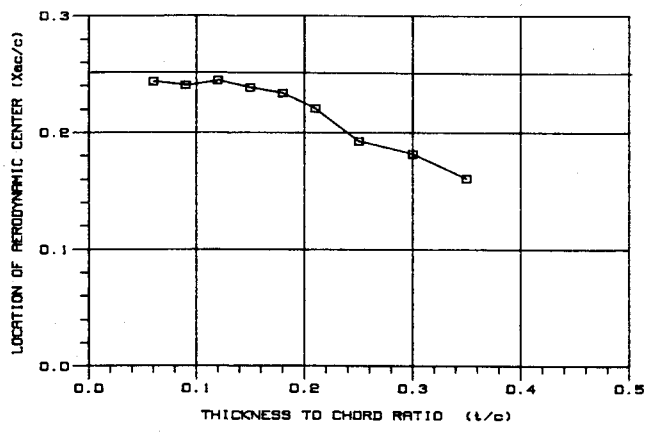

Fig. 2 NACA 00XX aerodynamic center.

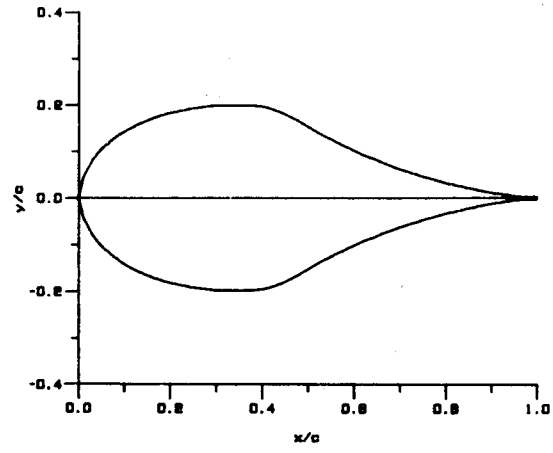

Liebeck 40% Section Profile

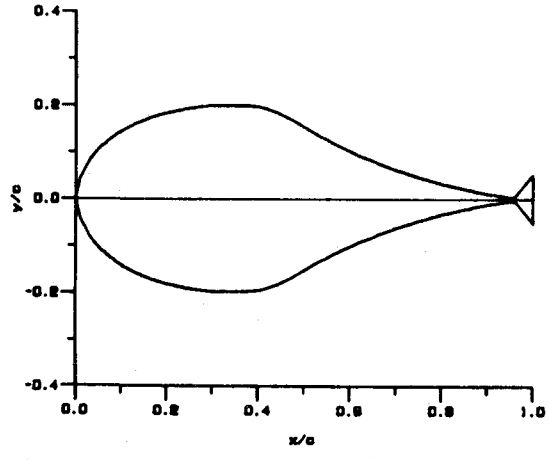

Liebeck 40% Section Profile with Trailing Edge Wedge

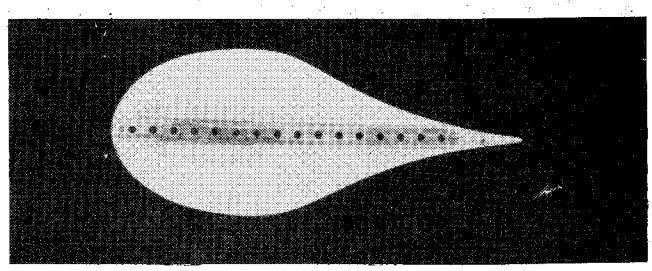

Fig. 3 Liebeck baseline section ($t/c = 0.4$).

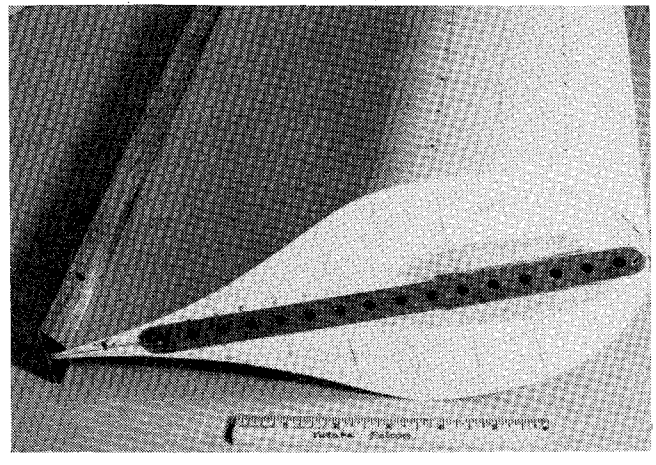

Fig. 4 Baseline section/trailing-edge wedge.

great enough to avoid cavitation, the aerodynamic characteristics will be the same as the hydrodynamic characteristics. The tests were conducted in the University of Washington "Venturi" open-return-type wind tunnel, which has an octagonal cross section of 0.9 m across the vertices. With a maximum speed of 27 m/s, a fairing section model with a 30.5 cm chord may be operated at Reynolds numbers up to 5×10^5. The operational Reynolds number range for faired cables is from 5×10^4 to 1×10^6, while it is about $2\text{-}5\times10^6$ for faired riser pipes.

Using the sphere drag coefficient method, the wind-tunnel turbulence level has been measured at 2.15%, which is equivalent to a turbulence factor of 2.85. In general, the turbulence intensity in the ocean will vary with location and depth. The ocean turbulence level is difficult to measure directly; however, the turbulent rms velocity fluctuations may be computed based on measurements of the rate of velocity fluctuation viscous dissipation. The turbulence level may then be computed by dividing the velocity fluctuations by either the towing or current velocity. For a towing speed of 5 m/s, the resulting turbulence intensities vary 0.09-27% over a depth range of 0-750 m in one location and 0.6-8.7% over a depth range of 0-23 m in another location. Because of this wide range of variation in turbulence intensity, the wind-tunnel data are presented as measured.

The Liebeck "Stratford pressure recovery section" (Fig. 3), with t/c reduced to 0.4, was selected as the baseline configuration for the initial investigation. The trailing-edge wedge had a length of 0.05 chord with an included angle of 90 deg, see Fig. 4. The vortex generator configuration (Fig. 5) was based on the recommendations of Pearcey,[7] where the length l, height h, and spacing d were 0.01, 0.025, and 0.1 chord, respectively. The vortex generators were fabricated in the form of a continuous strip that could be positioned at any station along the chord.

The two-dimensional model was mounted in a vertical position between the top and bottom of the wind tunnel and was free to rotate about a pivot aligned with the leading edge. The pivot position was variable along the section chord, with the center of rotation positions at 5% chord stations along the chord. The model, with a 30.5 cm chord and 0.84 m span b is shown in the wind-tunnel installation in Fig. 6. The following measurements were made:

1) Determination of position of hydrodynamic center or neutral stability point, which was accomplished by progressively moving the pivot point back from the leading edge until a static yaw angle other than 0 deg was obtained. The position of the pivot point for this condition was the location of the hydrodynamic neutral stability point.

2) Torque about the center of rotation as a function of yaw angle.

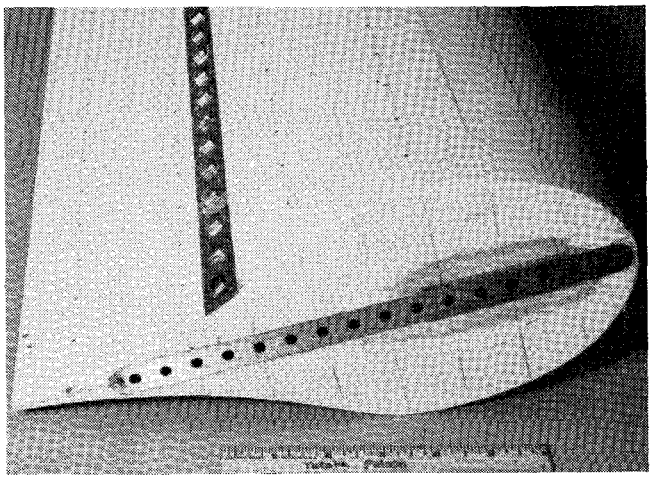

Fig. 5 Baseline section/vortex generators.

3) Wake survey to determine two-dimensional section drag coefficient.

4) Boundary-layer visualization to determine positions of the laminar-to-turbulent transition and the laminar or turbulent separation.

The wake rake, shown in Fig. 6, was positioned at mid-tunnel height, 0.75 chord length downstream of the model trailing edge. This position was determined experimentally to be where the static pressure was constant across the wake and equal to the upstream static pressure. At a spacing of 1.27 cm (total width = 25.4 cm), 35 total head and 10 static probes were used for the wake rake.

The wake data were corrected for blockage in the following manner. The blockage correction factor was first determined experimentally as

$$\epsilon=\frac{V_0}{V_\infty}-1=\frac{\Delta V}{V_\infty} \tag{1}$$

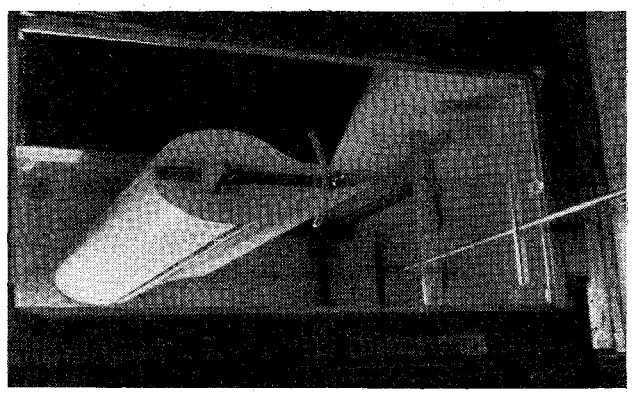

Fig. 6 Wind-tunnel installation.

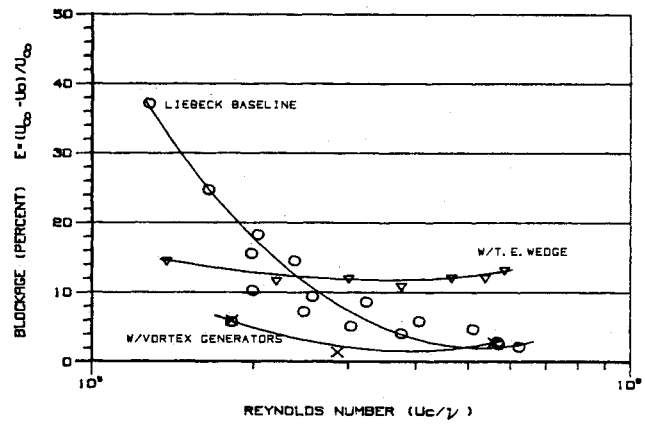

Fig. 7 Liebeck sections in wind-tunnel blockage.

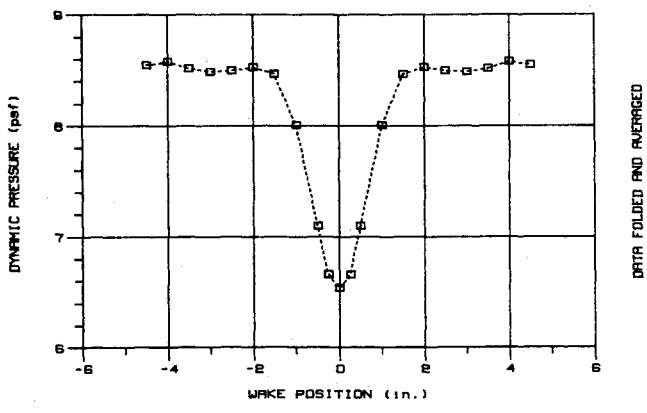

Fig. 8 Baseline/wake survey ($R_e=5.1\times10^5$).

where V_∞ is the upstream velocity and V_0 the downstream velocity at edge of wake.

The blockage correction factors are shown in Fig. 7 as a function of the Reynolds number based on V_0. Blockage over the Reynolds number range tested varies from 37% down to 2% for the baseline model, while it was constant at about 13% for the trailing-edge wedge configuration. The addition of the vortex generators to the baseline model decreased the blockage due to modification of the boundary layer. A typical baseline model wake profile for a Reynolds number of 5.1×10^6 is shown in Fig. 8. The symmetry of the profile is due to port and starboard averaging of the data.

The drag coefficient was then computed using the NASA method described by Shaw et al.,[8] which includes the blockage correction factor,

$$C_d=\frac{2}{c}\int\left[\left(\frac{V}{V_\infty}-\epsilon\right)\left(1-\frac{V}{V_\infty}+\epsilon\right)\right]dy \qquad (2)$$

where V is the wake velocity and dy the distance across wake.

Two techniques were used for flow visualization, including fluorescent minitufts[9,10] and the oil/ultraviolet light method. The fluorescent minituft technique developed by Crowder[9,10] utilizes extremely thin fluorescent nylon monofilaments having a diameter of about 0.018 mm. The minitufts were attached to the model surface with a drop of a lacquer-type adhesive. The use of the minitufts results in negligible interference with the flow, as determined by wind-tunnel tests[9,10]; consequently, a large matrix of tufts may be used for flow visualization. The tufts are used to map the areas of turbulent boundary-layer separation. The tufts, approximately 2.5 cm in length, must be viewed under ultraviolet light to contrast them with the model surface. A matrix of the tufts was applied at 10% chord stations along the chord with approximately equal spacings along the span of the model. With a white model background viewed under ultraviolet light, the model surface disappeared and the tufts were illuminated.

The second technique, which involved the use of oil and ultraviolet light, was used to determine the position of transition from laminar to turbulent flow in the boundary layer and the existence of a laminar separation bubble and turbulent separation. The latter thus serves as a check on the fluorescent minituft method. A mixture of kerosene (70% by volume), 10W40 motor oil (20%), and vinegar (10%) was used, along with approximately 9-10 cm^3 of fluorescent yellow pigment per 473.2 cm^3 of the liquid. The kerosene provides the base for the mixture, the motor oil slows down the rate of evaporation of the kerosene in the wind stream, and the vinegar is used to keep the powdered fluorescent pigment in suspension. It has been found through experiments that a lemon yellow pigment used in combination with a white model background results in the highest contrast.

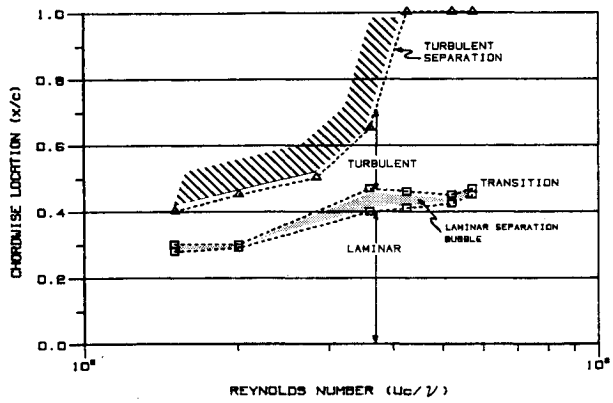

Fig. 9 Baseline/boundary-layer survey.

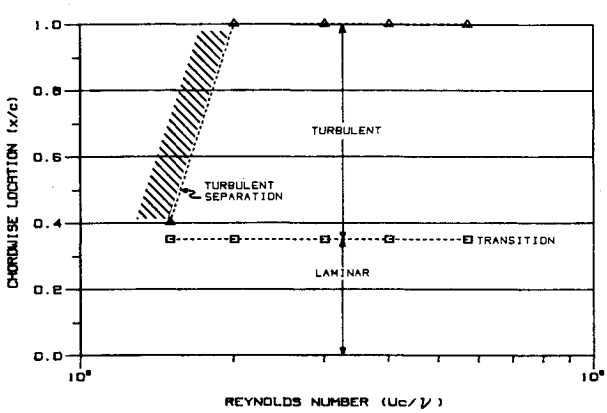

Fig. 10 Vortex generators/boundary-layer survey.

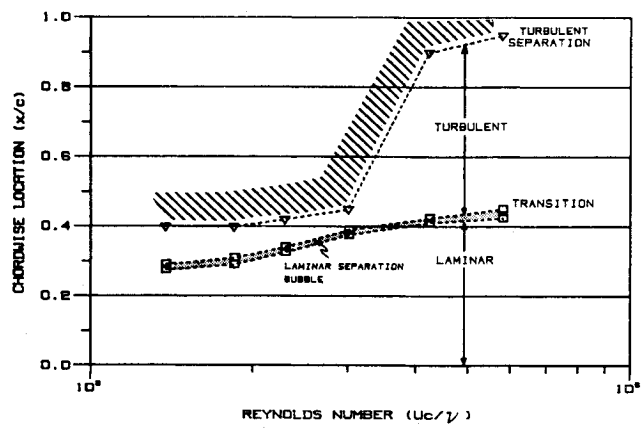

Fig. 11 Trailing-edge wedge/boundary-layer survey.

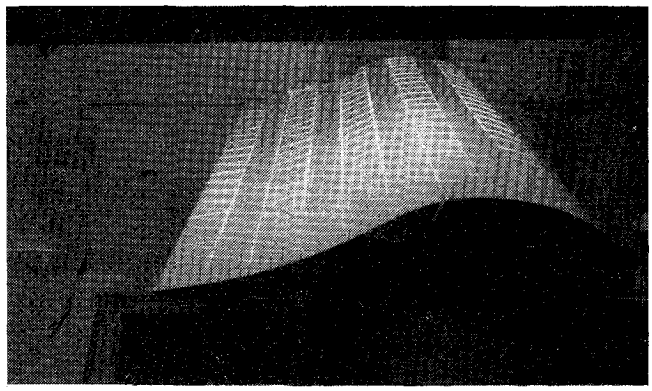

Fig. 12 Baseline/minitufts ($R_e=3.9\times10^5$).

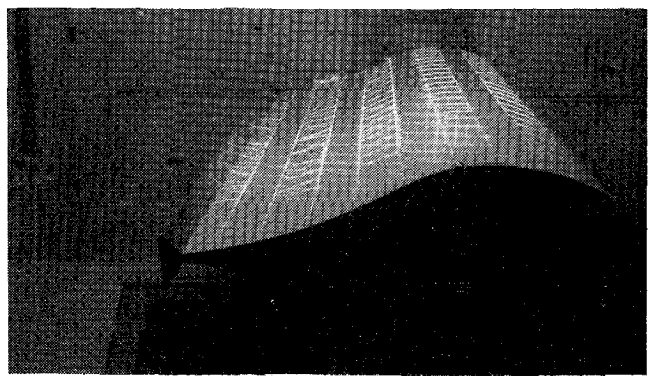

Fig. 13 Trailing-edge wedge/minitufts ($R_e=3.9\times10^5$).

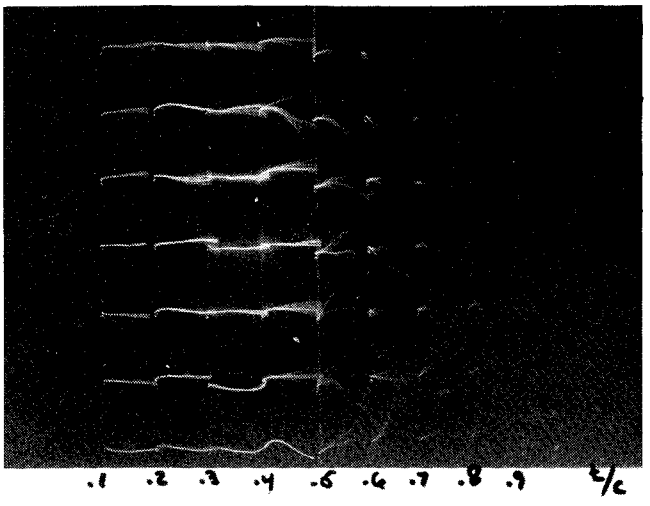

Fig. 14 Baseline/minitufts ($R_e = 2.5 \times 10^5$).

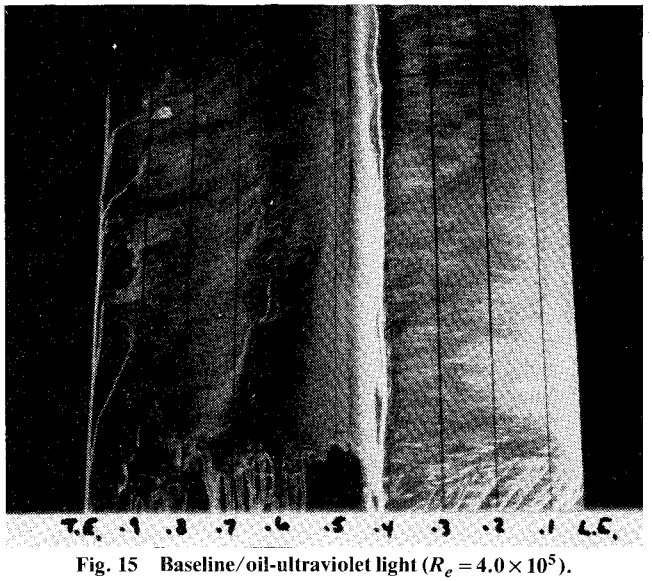

Fig. 15 Baseline/oil-ultraviolet light ($R_e = 4.0 \times 10^5$).

Both types of flow visualization were viewed under 100 W ultraviolet lights approximately 0.5-1.0 m from the model. Photography was accomplished with settings of f/2-f/4 at 1/15-1/30 s, using a Minolta ultraviolet light filter over a Griffin 1-A skylight filter.

Results

Boundary Layer

The results of both boundary-layer visualization surveys for all three model configurations are shown in Figs. 9-11 as a function of Reynolds number. Noted are the chordwise position of the transition from laminar to turbulent boundary layer and the existence of a laminar separation bubble and turbulent boundary-layer separation. A laminar separation bubble was found to exist at the transition from laminar to turbulent flow. The position of this laminar separation bubble coincided approximately with the point of minimum pressure coefficient, which is about 40% of the chord. It is seen from Fig. 9 that past a Reynolds number of 2.7×10^5, the turbulent separation over the aft portion of the section has completely disappeared. At the lower Reynolds numbers, approximately $1\text{-}2.7 \times 10^5$, the aft portion was separated from about 40% chord on. The results of the minituft and oil studies to indicate turbulent separation agree closely (Fig. 9). The boundary-layer studies were conducted simultaneously on either side of the model.

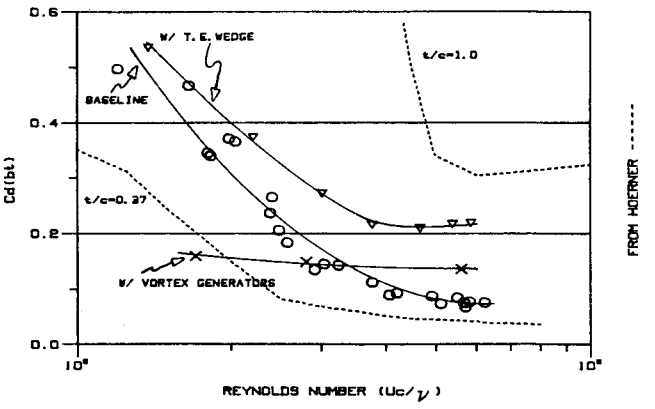

Fig. 16 Two-dimensional drag coefficient.

The vortex generators, which were fixed at 0.4 c, eliminated the turbulent separation at all but the lowest Reynolds number, as shown in Fig. 10. The addition of the trailing-edge wedge (Fig. 11) had no effect except at the higher Reynolds numbers. A standing vortex flow was generated in the region of the wedge, such that a turbulent boundary separation condition was initiated. In all three cases, the transition from laminar to turbulent flow occurred at the same location. Transition occurred at 0.25 c for the low Reynolds number of 1×10^5 and moved progressively aft to 0.42 c at 5.5×10^5. The effect of the massive turbulent separation at $1\text{-}2.7 \times 10^5$ apparently caused this migration forward.

The results of the fluorescent minituft survey (Figs. 12 and 13) show the fully attached flow for the baseline configuration at a Reynolds number of 3.9×10^5, and the effect of the standing vortex on the trailing-edge wedge flow pattern. The separated flow condition that existed for a Reynolds number of 2.5×10^5 is shown in Fig. 14. Separation starts at approximately the 40% chord position, after which the motion of the minitufts is quite dramatic. The oil technique results are shown in Fig. 15 for a Reynolds number of 4.0×10^5. The beginning of the laminar separation bubble can be seen at the 40% chord station. The fully attached turbulent boundary layer aft of this location can be distinguished from the laminar boundary layer forward of this location by the relative contrast between the pigment coating that remains on the surface. Since the shearing stress levels are lower in the laminar boundary layer, less of the oil is scrubbed away and, consequently, the yellow pigment has a much higher contrast in this area. In the turbulent boundary layer, the shearing stress levels are higher and consequently more of the liquid is scrubbed away, resulting in a darker area.

Drag Coefficient

The two-dimensional drag coefficient corrected for blockage for the three configurations tested is shown in Fig. 16 as a function of the Reynolds number based on chord. In order to provide a comparison, the results from Hoerner[11] are included for symmetrical sections with thickness/chord ratios of 37 and 100% (circular cylinder). It should be noted that the drag coefficient is based on the projected frontal area rather than the planform area. The shape of the baseline section curve is seen to agree well with the Hoerner curve. The drag coefficient decreases down to a Reynolds number of 4.0×10^5, after which it is approximately constant.

The addition of the vortex generators, which eliminated the boundary-layer separation at the low Reynolds number, is shown to decrease the drag coefficient in this region. The crossover point occurs at a Reynolds number of about 3.0×10^5, which agrees with the results shown in Fig. 9 where the turbulent separation disappeared on the baseline model.

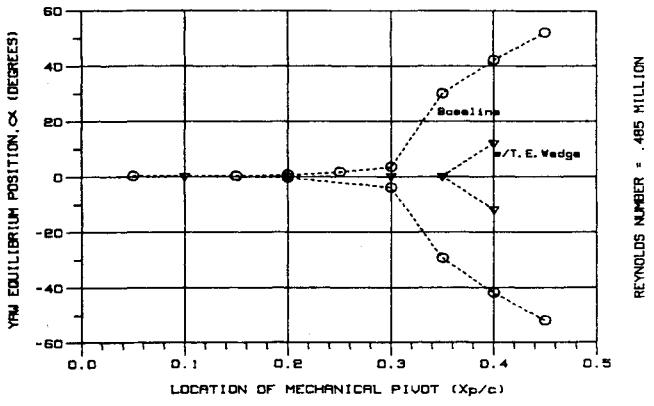

Fig. 17 Hydrodynamic center location.

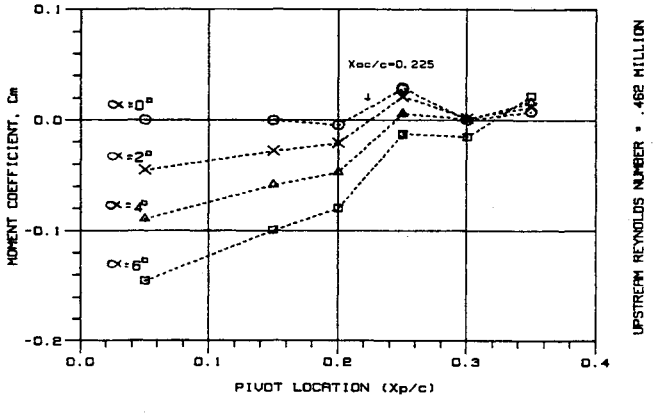

Fig. 18 Pivot point torque coefficient.

At Reynolds numbers above this point, the model with the vortex generators had a higher drag coefficient, indicating that the drag of the vortex generators themselves was quite large when working in a Reynolds number range where they had no effect on the boundary layer.

The addition of the trailing-edge wedge is seen to increase the drag coefficient over the entire Reynolds number range. At the higher Reynolds numbers, the drag coefficient is higher by a factor of three.

Hydrodynamic Center

The results of the hydrodynamic center (neutral point) location study are shown in Fig. 17 for a Reynolds number of 4.7×10^5. As can be seen for the baseline section, the hydrodynamic center is at about 20% of the chord. For pivot positions aft of this station, the model would assume a bistatically stable position at either a plus or a minus yaw angle, depending on which way the initial disturbance was directed. The unstable region increases until finally, beyond stations at approximately 30% of the section chord, it widely diverges.

The effect of adding the trailing-edge wedge is dramatic, as shown in Fig. 17. The model is seen to be stable for pivot positions all the way up to 35% of the chord, beyond which it was bistatically unstable. This indicates that the addition of the trailing-edge wedge would allow the use of a larger diameter cylinder. The penalty to be paid for this, of course, is the higher drag coefficient over the operating Reynolds number range.

Restoring Torque

The restoring torque coefficient, where

$$C_m = T/qbc^2 \tag{3}$$

is shown in Fig. 18 as a function of pivot location along the chord length for each yaw angle. The point where each curve crosses the zero moment axis corresponds to the neutral point position. At small angles of attack ($\leq$2 deg), this position corresponds with the data of Fig. 17.

Future Studies

This paper is a progress report on a continuing study. The relative merits of the two geometric approaches to separation-resistant sections, i.e., concave vs convex after sections, will be studied, as well as a range of thickness/chord ratios. The use of a trip wire instead of vortex generators and a reduction in the size of the trailing-edge wedge to reduce drag will be pursued.

The drag results presented here represent the two-dimensional characteristics of the fairing section and do not account for the end flow effects through the gaps between the relatively short lengths of fairing. After additional two-dimensional studies of other fairing sections are conducted, three-dimensional studies will be pursued.

Acknowledgments

This research was carried out under the Naval Sea Systems Command General Hydromechanics Research Program administered by the David W. Taylor Naval Ship Research and Development Center, under Office of Naval Research Contract N0014-82-K-0006.

References

[1] Chadakoff, R., "Plastic Clam Shells," *Popular Science,* Nov. 1978, p. 20.

[2] Henderson, J. F., "Some Towing Problems with Faired Cables," *Ocean Engineering,* Vol. 5, 1978, pp. 105-125.

[3] Eastman, N. J. and Abbot, I. H., "Airfoil Section Data Obtained in the NACA Variable-Density Tunnel as Affected by Support Interference and Other Corrections," NACA Rept. 669, 1939.

[4] Grant, R. and Patterson, D., "Riser Fairing for Reduced Drag and Vortex Suppression," Paper 2921, Offshore Technology Conference 1977.

[5] Smith, A.M.O., "High-Lift Aerodynamics," AIAA Paper 74-939, 1974.

[6] Thieme, H., "Design of Ship Rudders (Zur Formgebung von Shiffsrudern)," translated by E. N. Labouvie, U.S. Dept. of the Navy, Trans. 321, Nov. 1965.

[7] Lachmann, G. V., *Boundary Layer and Flow Control, Its Principles and Application,* Vol. 2, Pergamon Press, New York, 1961.

[8] Shaw, R. J., Sotos, R. G., and Solano, F. R., "An Experimental Study of Airfoil Icing Characteristics," AIAA Paper 82-283, 1982.

[9] Crowder, J. P., Hill, E. G., and Pond, C. R., "Selected Wind Tunnel Testing Developments at the Boeing Aerodynamics Laboratory," *Proceedings of AIAA 11th Aerodynamic Testing Conference,* March 1980, AIAA Paper-80-0458-CP.

[10] Crowder, J. P., "Add Fluorescent Mini-tufts to the Aerodynamicist's Bag of Tricks," *Astronautics & Aeronautics,* Vol. 18, Nov. 1980, pp. 54-56.

[11] Hoerner, S. F., "Fluid-Dynamic Drag," Hoerner Fluid Dynamics, Brick Town, N.J., Vol. 18, pp. 54-56.